*Available online www.jocpr.com*

**Journal of Chemical and Pharmaceutical Research, 2015, 7(9S):139-146**


**Research Article**

**ISSN : 0975-7384**
**CODEN(USA) : JCPRC5**

# Preparation, characterization of $ZnO/CoFe_2O_4$ magnetic nanocomposites and activity evaluation under solar light irradiation

**Rahmayeni*, Devi A., Yeni Stiadi, Novesar Jamarun, Emriadi and Syukri Arief**

*Department of Chemistry, Faculty of Mathematics and Natural Sciences, Andalas University, Padang, Indonesia*

---

**ABSTRACT**

*In this study, an attempt was made to prepare the magnetic nanocomposites of $ZnO/CoFe_2O_4$ by sol-gel process followed hydrothermal method and used as photocatalyst for degradation of dye in water. The crystal phase, surface morphology, chemical composition and magnetic properties were investigated by XRD, FESEM-EDX and VSM, respectively. The photocatalytic activities of the as-prepared sample have been evaluated by photodegradation of Rhodamin B under solar light irradiation. The SEM image showed that the nanocomposites composed of rod-like particles. The specific peaks of XRD pattern of nanocomposites correspond to the spinel cubic of $CoFe_2O$ and hexagonal wurtzite of ZnO. The magnetic properties of $ZnO/CoFe_2O_4$ nanocomposites exhibit a ferromagnetic behavior, which is useful for the separation and it could be reuse after photocatalytic process. All of nanocomposites exhibited higher photocatalytic activity than pure ZnO, and at 1:0.01 molar ratio of ZnO to $CoFe_2O_4$, the obtained product showed the highest photocatalytic activity.*

**Keywords:** $ZnO/CoFe_2O_4$, magnetic, photocatalyst, sol-gel, hydrothermal

---

## INTRODUCTION

Semiconductor material has been widely used as photocatalyst in as much as various organic pollutants can be easily degraded under UV or solar light irradiation [1]. Extensively investigations were carried out worldwide to decompose the organic pollutants using semiconductor type photocatalyst like $TiO_2$ and ZnO [2]. ZnO nanostructures have been extensively studied as photocatalyst because of many interesting properties such as its wide direct band gap of 3.37 eV, high exiciton binding energy at room temperature, favorable chemical and thermal stabilities [3]. As a very important semiconductor material, ZnO can be used in many fields such as solar cell [4], sensors [5-6], sunscreen [7], and self-cleaning [8].

Some research works have revealed that nanoscale of ZnO as photocatalyst exhibit superior advantages than $TiO_2$ which is ascribed to the lower cost, higher quantum efficiency, environmental friendliness and biodegradable [9]. Moreover, ZnO has concerned because it generates $H_2O_2$ more efficiently in detoxification process due to it has more numbers of the active site with high surface reactivity hereby increasing the reaction and mineralization rates [10]. However, the wide band gap limits its absorption to the UV region which occupies less than 10 % of solar spectrum [11]. Various effort have been made to modify the band gap of ZnO to improve the photocatalyst property by combine with other elements [10, 12-17], metal oxides [18-21] sensitizing with narrow band gap semiconductor [1-2, 9, 22-25] and grafting heteronanostructure [9].

In other hand, spinel ferrites, including $CoFe_2O_4$, are an important magnetic due to interesting properties with large magnetic anisotropy, moderate saturation magnetization, remarkable stability and mechanical hardness [2]. Ferrites materials have been widely used in many applications, such as in electronic devices, information storage, magnetic resonance imaging and drug delivery technology [26]. In addition, the band gap of $CoFe_2O_4$1.17 eV, which means the $CoFe_2O_4$ nanoparticles can be considered as the low band gap semiconductor that enhance the visible light responsive photoactivity [3;11]. They are seldom used as photocatalyst independently due to the lower valence band potential and poor property in photoelectric conversion [1]. Combining the two materials, ZnO and CoFe2O4, can lead to visible light responsive photocatalyst as well as magnetically active. In the presence of magnetic materials, the nanophotocatalyst can be easily separated and collected with an external magnetic field from an aqueous suspension which prevents the secondary pollution created by the disposal of photocatalyst [27-28]. The modification ZnO semiconductor with $CoFe_2O_4$ using several methods have been reported, for instance, coprecipitation [11], two-step hydrothermal route with the assistance of the template [3;29], combustion reaction [30], collosol [31], sono-chemical route [23], and conventional ceramic [32].

In this paper, we report the preparation of ZnO/$CoFe_2O_4$ magnetic nanocomposite by sol-gel process followed hydrothermal method and used as photocatalyst for degradation of dye in water. The photocatalytic activities were evaluated by degradation of Rhodamin B under natural solar light.

## EXPERIMENTAL SECTION

### Materials

Cobalt nitrate ($Co(NO_3)_2.6H_2O$), Ferric nitrate ($Fe(NO_3)_3.9H_2O$), Zinc nitrate ($Zn(NO_3)_2.4H_2O$) citric acid, ethanol ($C_2H_5OH$), potassium hydroxide (NaOH) and Rhodamin B were purchased from the Merck. Solution was prepared using distilled water.

### Preparation of the ZnO/$CoFe_2O_4$ Nanocomposites

First, the $CoFe_2O_4$ spinel nanoparticles were prepared by sol-gel method. Measured amount of $Co(NO_3)_2.6H_2O$ and $Fe(NO_3)_3.9H_2O$ with molar ratio 1:2 were dissolved in certain amount of ethanol under stirring. The mixture was added by citric acid solution using ethanol as the solvent. The solution was kept under stirring and heated at 70$^o$C for 1 hour. When the solution became viscous, the gel was formed and later taken out and dried at 100$^o$ C for 24 hour to obtain the dry gel. The residual precursor was calcined at 500$^o$ C for 2 hour to form $CoFe_2O_4$ nanoparticles. Second, the nanocomposite of ZnO/$CoFe_2O_4$ was prepared by hydrothermal method as follow procedure, 20mmol of $Zn(NO_3)$ 2.4 $H_2O$ and $CoFe_2O_4$ nanoparticles mixed into 40mL of distilled water with a variation of percentage mole ratio of $Zn^{+2}$: $CoFe_2O_4$ is 1:0.1,1: 0.05; and 1: 0.1(named by NCo-1, NCo-2, and NCo-3). Then NaOH (2M) solution was added drop wis eto the mixture until the pH to 12. The mixture was put into an autoclave and heated for 3 hours at 180$^o$ C. The obtained ZnO/$CoFe_2O_4$ powder were filtered and washed with distilled water until neutral pH, then dried at70 °C for 2 hours. For comparison, ZnO was also prepared by the hydrothermal method.

### Characterization

The phase identification and crystalline structure analysis were determined by X-Ray Diffraction using XPERT-PRO *Diffractometer system*. Surface morphology were analyzed by Field Emission Scanning Electron Microscopy (FEI Inspect F50), the magnetization measurement were performed by OXFORD 1.2H Vibrating Sampler Magnetometer.

### Evaluation of Photocatalytic Activity

The photocatalytic activities of prepared samples were evaluated by degradation of Rhodamin B dye under solar light irradiation. Photocatalysts (20 mg) were added to 20 mL Rhodamin B solution (10 mg/L) and then the aqueous suspension was stirred to obtain better dispersion. Irradiation of sunlight is used directly for the suspension with interval time 1 h. Thereafter, the sample solution is analyzed by a spectrophotometer at a wavelength of 553 nm to determine the amount of degraded Rhodamin B. For comparison ZnO, $CoFe_2O_4$ was also used for photocatalytic evaluation. The photocatalytic degradation percentage was calculated using followed equation:

$$\text{Degradation } \% = \frac{A_{0-}\, A}{A_0} \times 100\%$$

## RESULTS AND DISCUSSION

### Structure and Morphology of samples

Fig. 1 shows the XRD pattern of (a) pure $CoFe_2O_4$ (b) pure ZnO and ZnO/$CoFe_2O_4$ nanocomposites obtained with different contents of $CoFe_2O_4$; (c) NCo-1, (d) NCo-2 and (e) NCo-1.

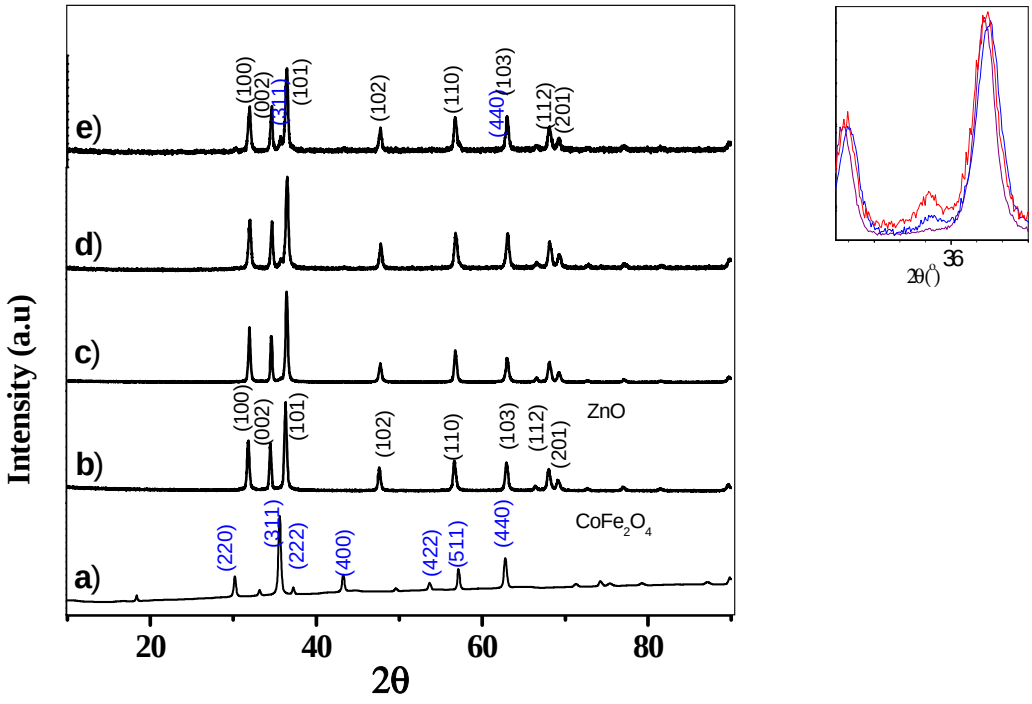


**Figure 1. XRD Pattern of (a) $CoFe_2O_4$, (b) ZnO, (c) NCo-1, (d) NCo-2, (e) NCo-3 and the insert shows the specific peak of $CoFe_2O_4$ at 2θ of 35.7°**

X-ray diffraction patterns of samples are shown in Fig.1. The XRD pattern of $CoFe_2O_4$ (fig. 1a) exhibit clear specific peaks at 2θ of 30.2°, 35.7°, 37.2°, 43.3°, 53.6°, 57.1°, and 62,7° corresponding to (220), (311), (222), (400), (422), (511), (440) planes (ICDD #01-076-7254). The small impurity was observed at 2θ of 33.1°correspond to $Fe_2O_3$. In the insert on the Fig. 1. shown the expanded region of $CoFe_2O_4$ around 2θ of 35.7°in nanocomposites. It can be seen that the peak intensity increase as increasing the contents of $CoFe_2O_4$ in nanocomposites. This indicates that relative intensities as well as the angular positions of the XRD peaks associated to both single-phased materials are systematically changing as the ferrite content increases [23]. Fig. 1b) show The wurtzite structure of ZnO with specific peaks at 2θof31.8°, 34.5°, 36.2°, 47.5°, 56.6° , 62.8°, and 68°can be indexed to (100), (002), (101), (102), (110), (103), (200) planes. The XRD pattern of nanocomposite shows peaks almost match only one peak of $CoFe_2O_4$. The specific peak at 35,7° that corresponds to 311 plane indentifies the presence $CoFe_2O_4$ in nanocomposite and not influence any changes on the crystal structure.

FESEM analysis of $CoFe_2O_4$ and ZnO/$CoFe_2O_4$ nanocomposite are represented in Fig. 2. NCo-1 was chosen because it shows the best photocatalytic activity compared the others. It is evident from FESEM analysis that the particle size of $CoFe_2O_4$ have a spherical shape and have a low aggregates. ZnO morphology is represented in Fig. 2 (c-d). Particles have rod-like shape and uniform. The corresponding EDX analysis of the samples is shown in Fig.3. respectively. Figure 3-a shows the element content exhibit the Co, Fe, O peaks only which reflects the atomic ratio of the respective nanoparticles. Analyis EDX (Figure 2-f) of the NCo showed absence $CoFe_2O_4$ element in the nanocomposite. It is estimated that this happens because of the uneven spread of elements and the amount of$CoFe_2O_4$ very small.

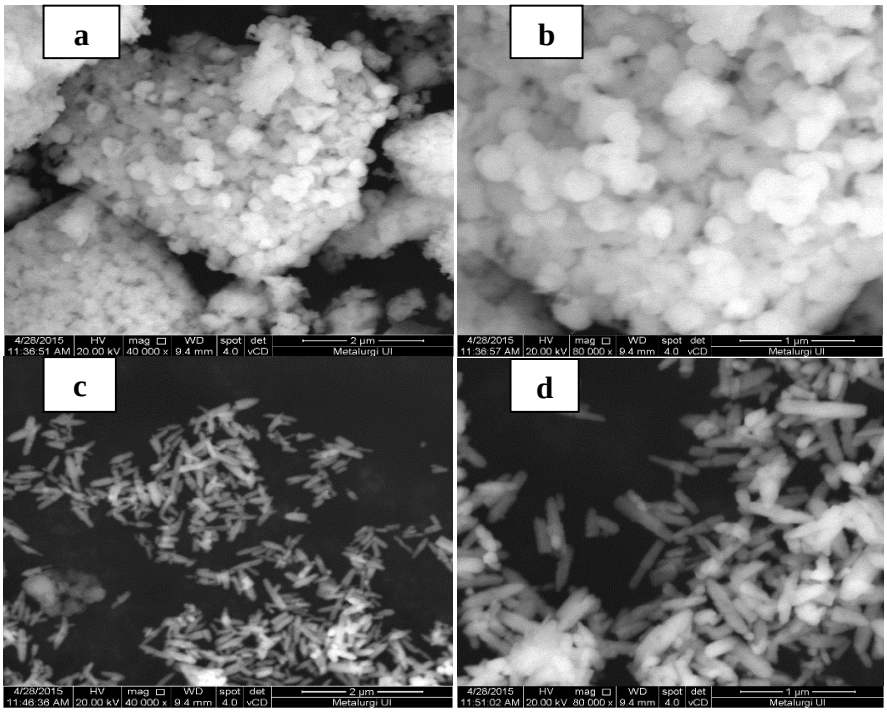


**Figure 2. FESEM Image of $CoFe_2O_4$ (a-b), NCo-1 (c-d)**

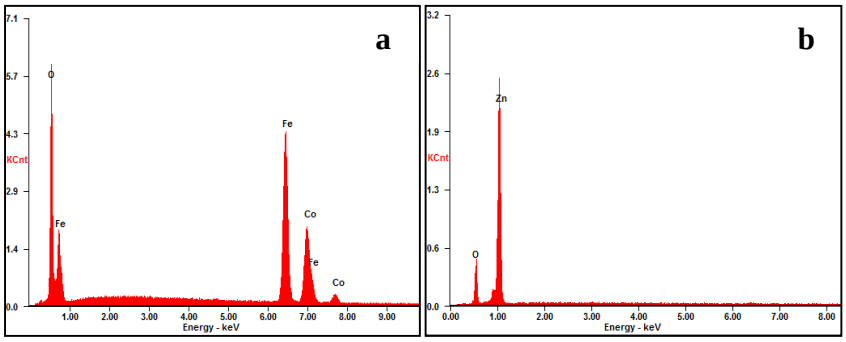


**Figure 3. EDX spectra of $CoFe_2O_4$ (a) and NCo-1 (b)**

**Magnetic Properties**

Magnetic properties of the synthesized photocatalyst were studied at room temperature as shown in Fig.4. The magnetic hysteresis loop clearly indicates that $CoFe_2O_4$ nanoparticles are more magnetically active than nanocomposites (Fig. 4A). From magnetic saturation value (MS), these particles showed the strong ferromagnetic properties. In the other hand, nanocomposites NCo have a lower ferromagnetic properties (Fig. 4B). It is due to ZnO is diamagnetic reduce the magnetic properties of $CoFe_2O_4$. However, the nanocomposites containing magnetic behavior have profit due to separate easily from liquid by the application of external magnetic field after applied and can be used for the next application and of course avoids the hazardous disposal of photocatalysts to the environment.

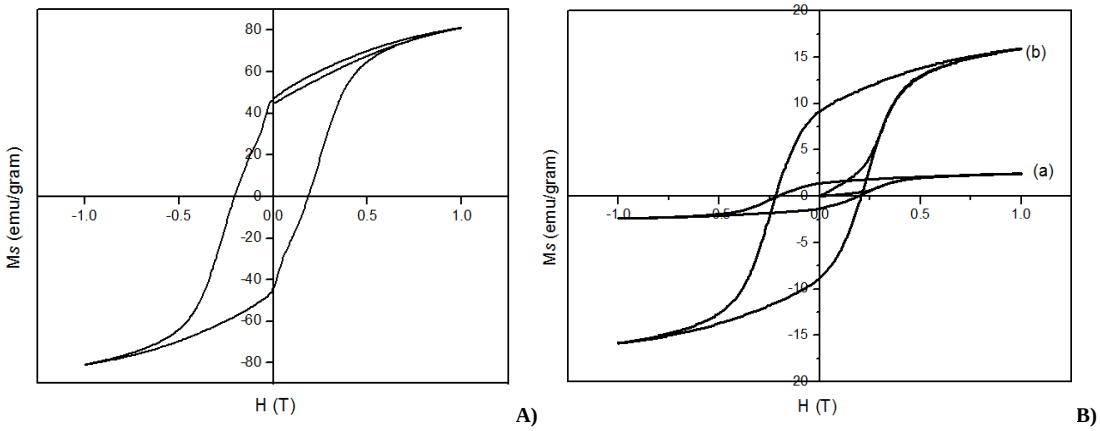


**Figure 4. Magnetizationhysteresis loops of A) $CoFe_2O_4$ and B) $ZnO/CoFe_2O_4$ (NC-1 a, NC-2 b)**

**Evaluation of Photocatalytic Activity**

Degradation percentage of Rhodamin B in the presence of pure ZnO and $CoFe_2O_4$, and $ZnO/CoFe_2O_4$ nanocomposite under solar light irradiation are shown in Fig.5.It clearly seen that the degradation % of Rhodamin Bin the presence of NCo-1 reaches 98.76 %. It is achieves 30.21% higher when compared to degradation in pure ZnO. The enhancement of the photocatalytic activity in $ZnO/CoFe_2O_4$ nanostructure may due to the formation of heterojunction in ZnO semiconductor interface can enhance charge separation of photo-generated e-/h+ pairs and improve the photocatalytic efficiency. $CoFe_2O_4$ nanoparticles are known as a p-type semiconductor and metal doped-ZnO (metal = Co, Fe) is a n-type semicondustor. $CoFe_2O_4$ with a band gap of 1.17 eV has a smaller work function when compared to the work function of ZnO (3.2 eV) that the Fermi energy level of ZnO is lower than $CoFe_2O_4$. A negative shift in the Fermi level of ZnO and positive shift in the Fermi level of ZnO are expected when the band edges of the $CoFe_2O_4$ at the interface shift to appropriate the Fermi level until equilibrium is reached. At the interface, an inner field is formed that causes the electron move from ZnO region to $CoFe_2O_4$ leaving the ZnO region with positive charges and the $CoFe_2O_4$ region with negative charges. When the $CoFe_2O_4$–ZnO heterojunction was excited by higher or equal photon energy to the band gaps of ZnO and $CoFe_2O_4$, the electrons in the valence band (VB) moved to the conduction band (CB) generating equal amount of holes in VB. This process transfers the photogenerated electrons from the CB of $CoFe_2O_4$ to the CB of ZnO. Conversely, the photogenerated hole transfer takes place from the VB of ZnO to the VB of $CoFe_2O_4$. This suggests that the photogenerated electrons and holes in the heterojunction were efficiently separated. The excess valance band electrons then migrate to the surface of ZnO and react with the trapped O2 to produce superoxideradical anions,O2•−, which on protonation generates •OH. Similarly, the holes that were transferred to the $CoFe_2O_4$ react with the trapped by surface hydroxyl groups (or H2O) in $CoFe_2O_4$ to yield •OH radicals. These •OH radicals is highly reactive to degrade organic molecules and can enhance the photocatalytic activity of the sample. The as-prepared $CoFe_2O_4$–ZnO nanostructure combined the catalytic and magnetic properties, which could be isolated from the reaction mixture easily using an external magnet at the end of the reaction and recycled without loss of catalytic activity [23].

The percentage degradation of Rhodamin Bwas decreased as its $CoFe_2O_4$ content increases up to molar ratio value of 1:0.1. This phenomenon may be attributed to that both semiconductors, ZnO and $CoFe_2O_4$, are active under UV-Vis irradiation. This results in an increase in electron population in the CB of ZnO in which electrons are injected not only from the sensitizer but also excited from its own VB. ZnO can transfer its photogenerated holes to the sensitizer increasing the hole concentration in the VB of sensitizer. This accumulation of charge carriers increases the probability of electron–hole recombination which can significantly reduce the photocatalytic activity of coupled system. Since holes are left behind in the valence band of narrow band gap semiconductors they can photocorrode it if not engaged in redox reactions [34].

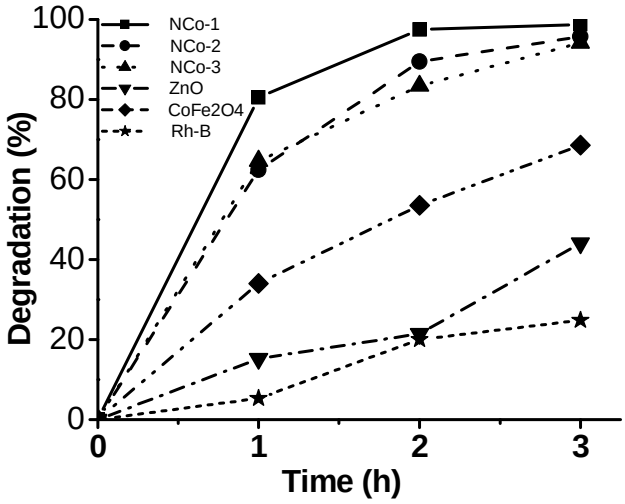


**Figure 5. Plot of degradation % of Rhodamin B upon radiation time in the presence of ZnO, $CoFe_2O_4$, NC-1, NC-2, NC-3 and without photocatalyst**

The maximum degradation observed for the NCo-1 was used as the optimized composition value for the optimizing further photocatalytic degradation parameter. Fig.5. shows effect of variation of photocatalyst loadingon the degradation % of Rhodamin B using NCo-1. The variation of photocatalyst loading was conducted from 0.25 g/L to 1 g/L. Based on the curve can be seen that at 1g/L photocatalyst loading the photocatalytic activity reach of 99.21%. It is not much different if compared with 0.75 g/L loading with degradation percentage of 98.99% during 3 hours irradiation.

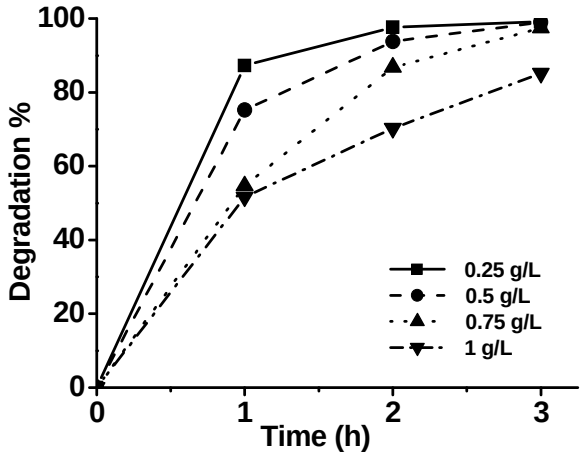


**Figure 6. The Effect of variation of photocatalyst loadingon the degradation % of Rhodamin Busing NCo-1**

Reusability of $ZnO/CoFe_2O_4$ nanocomposite as photocatalyst was evaluated. The photocatalyst was recycled after filtered, washed and dried. The dried photocatalyst were used for degradation of Rhodamin B, employing similar experimental conditions. The result of degradation efficiency was shown in table 1. Photocatalyst exhibit remarkable photostability as the Rhodamin B percentages are 99.68 % and 99.49% in the first and second runs, respectively for 3 hours. These results demonstrates that the photocatalyst was found to be very stable and did not lose its catalytic activity significantly therefore the synthesized photocatalyst were reusable.

**Table 1. Degradation % of Rhodamin B in the presence of initial and recycle of NCo-1**

| Time (hour) | Degradation (%) | |
|---|---|---|
| | initial | recycle |
| 0.5 | 58.15 | 54.69 |
| 1 | 82.69 | 70.97 |
| 1.5 | 91.75 | 92.96 |
| 2 | 95.21 | 96.12 |
| 2.5 | 99.04 | 97.35 |
| 3 | 99.68 | 99.49 |

## CONCLUSION

Nanocomposite photocatalysts of $ZnO/CoFe_2O_4$ were prepared using sol-gel process followed hydrothermal method successfully. XRD analysis indicates conformity with cubic spinel of $CoFe_2O_4$ and wurtzite structure of ZnO. Additions of $CoFe_2O_4$ to the construction ZnO managed to increase the photocatalytic activity in the visible light region so as to degrade the Rhodamin B under solar light irradiation. Their magnetic properties indicate that the $ZnO/CoFe_2O_4$ nanocomposites are potential as are usable photocatalyst.

## REFERENCES

[1]L Sun; R Shao; LQ Tang; C Zhidong. *J. Alloys and Compounds*, **2013**, 564, 55–62.
[2]NV Kaneva; CD Dushkin. *Colloids and Surfaces A: Physicochem. Eng. Aspects*, **2011**, 382, 211–218.
[3]L Ye; C Yan; Y Jiang; Q Yang, C Lu, W Guan. *Micro & Nano Letters*, **2015,** 10(4), 202–205.
[4]YF Zhu; DH Fan; YW Dong; GH Zhou. *J. Superlattices and Microstructures*, **2014**, 74, 261–272
[5]HS Al-Salman; MJ Abdullah; N Al-Hardan. *Ceramics International*, 2010, 35, 4428-4434
[6]CH Ashok ;KV Rao. *Superlattices and Microstructures*, **2014**,76, 46–54.
[7]TH Le; AT Bui; TK Le. *Powder Technology*, **2014**, 268, 173–176.
[8]HY He. *J. of Materials Science in Semiconductor Processing*, **2015**, 31, 200–208.
[9]NR Su; P Lv; M Li; X Zhang; M Li; J Niu, *Materials Letters*, **2014**, 122, 201–204.
[10]R Ullah; J Dutta. *J. of Hazardous Materials*, **2007**, 156, 194–200.
[11]P Sathishkumara; N Pugazhenthirana; R.V Mangalarajab; A.M Asiri; S Anandana. *J. of Hazardous Materials*, **2013**, 252–253, 171– 179.
[12] X Wu; Z Wei; L Zhang; X Wang; H Yang; J Jiang. *Hindawi Publishing Corporation Journal of Nanomaterials*, **2014**, 1-6.
[13] Y Liu;H Liu; Z Chen; N Kadasala; C Mao; Y Wang; Y Zhang; H Liu; Y Liu; J Yang; Y Ya. *Journal of Alloys and Compounds*, **2014,** 604, 281–285.
[14] M Rajbongshi; A Ramchiary; SK Samdarshi. *Materials Letters*, **2014,** 134, 111–114.
[15] N Kaneva; A Ponomareva; L Krasteva; D Dimitrov; A Bojinova; K Papazova; G Suchaneck; V Moshnikov. *Bulgarian Chemical Communications*, **2013**, 4(45), 635–643.
[16] R He; RK Hocking; T Tsuzuki. *J. of the Australian Ceramic Society*, **2013**, 1(49), 70–75.
[17] R Georgekutty; MK Seery; C Suresh; P Pillai. *J. Phys. Chem. C*, **2008**, 112, 13563–13570.
[18] MA Habib; MD Shahadat; NM Bahadur; M Ismail; A Jafar A; V Mahmood. *International Nano Letters*,**2013**, 3, 5-12.
[19] V Kuzhalosai; B Subash; A Senthilraja; P Dhatshanamurthi; M Shanthi. *Spectrochimica Acta Part A: Molecular and Biomolecular Spectroscopy*, **2013**, 115, 876–882.
[20] D Jassby; JF Budarz; M Wiesne. *Environ. Sci. Technol*, **2012**, 46, 6934−6941.
[21] NP Mohabansi; VB Patil; N Yenkie. *Rasayan Chemistry Journal*, **2011**, 4(4), 814-819.
[22] DD Qin; CL Ta. *The Royal Society of Chemistry*, **2014**, 4, 16968–16972.
[23] C Borgohain; KK Senapati; KC Sarma; P Phukan. *J. of Molecular Catalysis A*, **2012**, 363– 364, 495– 500.
[24] J Jiang; LH Ai; LC Li; H Liu. *J. of Alloys and Compounds*, **2009**, 484, 69-72.
[25] C Shifu; Z Wei Z; L Wei; Z Huaye; Y Xiaoling. *Chemical Engineering Journal*, **2009**, 155, 473-566.
[26] HS Qian; Y Hu; ZQ Li; XY Yang; LC L; XT Zhang; R Xu. *J. Phys. Chem. C*,**2010**, 114, 17455–17459.
[28] VK Gupta; T Eren; N Atar; ML Yola; C Parlak; HK Maleh. *Journal of Molecular Liquids*, **2015,** 208, 122–129.
[29] A Wilson; SR Mishra; R Gupta; K Ghosh. *Journal of Magnetism and Magnetic Materials*, 2012, 324, 2597–2601.

[30] TJ Castro; SW daSilva; F Nakagomi; NS Moura; A Franco Jr; PC Morais. *Journal of Magnetism and Magnetic Materials*, **2015**, 389, 27–33.
[31] G Zhang; W Xu; Z Li; W Hu; Y Wang. *Journal of Magnetism and Magnetic Materials*, **2009**, 321, 1424-1427.
[32] S Rehman; R Ullah; AM Butt; ND Gohar. *Journal of Hazardous Materials*, **2009**, 170, 560–569.